Thrombospondin-1 controls vascular platelet recruitment and thrombus adherence in mice by protecting (sub)endothelial VWF from cleavage by ADAMTS13

Arnaud Bonnefoy, Kim Daenens, Hendrik B. Feys, Rita De Vos, Petra Vandervoort, Jos Vermylen, Jack Lawler, and Marc F. Hoylaerts

The function of thrombospondin-1 (TSP-1) in hemostasis was investigated in wild-type (WT) and *Tsp1*$^{-/-}$ mice, via dynamic platelet interaction studies with A23187-stimulated mesenteric endothelium and with photochemically injured cecum subendothelium. Injected calcein-labeled WT platelets tethered or firmly adhered to almost all A23187-stimulated blood vessels of WT mice, but *Tsp1*$^{-/-}$ platelets tethered to 45% and adhered to 25.8% of stimulated *Tsp1*$^{-/-}$ vessels only. Stimulation generated temporary endothelium-associated ultralarge von Willebrand factor (VWF) multimers, triggering platelet string formation in 48% of WT versus 20% of *Tsp1*$^{-/-}$ vessels. Injection of human TSP-1 or thrombotic thrombocytopenic purpura (TTP) patient–derived neutralizing anti-ADAMTS13 antibodies corrected the defective platelet recruitment in *Tsp1*$^{-/-}$ mice, while having a moderate effect in WT mice. Photochemical injury of intestinal blood vessels induced thrombotic occlusions with longer occlusion times in *Tsp1*$^{-/-}$ venules (1027 ± 377 seconds) and arterioles (858 ± 289 seconds) than in WT vessels (559 ± 241 seconds, $P < .001$; 443 ± 413 seconds, $P < .003$) due to defective thrombus adherence, resulting in embolization of complete thrombi, a defect restored by both human TSP-1 and anti-ADAMTS13 antibodies. We conclude that in a shear field, soluble or local platelet-released TSP-1 can protect unfolded endothelium-bound and subendothelial VWF from degradation by plasma ADAMTS13, thus securing platelet tethering and thrombus adherence to inflamed and injured endothelium, respectively. (Blood. 2006;107: 955-964)

Introduction

Damage of healthy blood vessels triggers platelet recruitment to adhesive vascular ligands, resulting in plug formation and arrest of bleeding.[1] The current model describing the recruitment of flowing platelets involves subendothelial von Willebrand factor (VWF) and vascular collagens, which mediate platelet tethering, rolling, and finally firm adhesion.[2] Especially under high shear stress, VWF interacts both with the platelet GPIb/IX/V receptor complex and with the integrin receptor $\alpha_{IIb}\beta_3$ and participates in platelet aggregation, properties it shares with fibrinogen (Fg), the main ligand for $\alpha_{IIb}\beta_3$. The more recent finding that stable thrombi can form in arterioles of mice lacking both VWF and Fg indicated that other vascular or platelet ligands, such as fibronectin, can contribute to platelet adhesion and aggregation.[3,4]

Thrombospondin-1 (TSP-1) is a large homotrimeric glycoprotein of approximatively 450 kDa, synthetized by several cell types, including vascular endothelial cells, smooth muscle cells, and fibroblasts, and is present in the vessel wall matrix.[5] In plasma, it circulates in only very low concentrations (0.1-0.3 μg/mL); in platelets, however, it is abundantly stored in α-granules, from where it can be secreted during platelet activation yielding plasma concentrations up to 10 to 30 μg/mL.[6] Its complex multidomain structure enables TSP-1 to interact with many cell-adhesive receptors, including CD36, several integrins ($\alpha_v\beta_3$, $\alpha_{IIb}\beta_3$, $\alpha_2\beta_1$, $\alpha_3\beta_1$, $\alpha_4\beta_1$, $\alpha_5\beta_1$, and $\alpha_6\beta_1$), the integrin-associated protein (IAP) CD47, and the GPIb/IX/V complex, heparan sulfate, as well as with other adhesive glycoproteins, including Fg, VWF, laminin, fibronectin, and collagen.[7]

In vitro, TSP-1 has been demonstrated to potentiate platelet activation and to stabilize platelet aggregates,[8,9] and a molecular model for the stabilization of TSP-1–mediated platelet-platelet bonds has been advanced recently.[10] Through its interaction with IAP, TSP-1 triggers the activation of $\alpha_{IIb}\beta_3$ and $\alpha_v\beta_3$ integrins, and it synergizes with collagen to activate platelets via $\alpha_2\beta_1$.[11,12] The functional coupling between IAP and heterotrimeric G proteins of the G_i subclass[13] provides a model explaining the biological effects of IAP in a wide variety of systems. In addition, it was recently demonstrated that immobilized TSP-1 interacts with the platelet GPIb/IX/V complex, mediating firm platelet adhesion at elevated shear rates up to 4000 s^{-1} independent of VWF.[14] Finally, a role for TSP-1 and IAP in the

From the Center for Molecular and Vascular Biology, Laboratory of Morphology and Molecular Pathology, and Laboratory for Thrombosis Research, Interdisciplinary Research Center, Campus Kortrijk, University of Leuven, Belgium; Department of Pathology, Harvard Medical School, Boston, MA; INSERM, U 553; Institut de Formation et de Recherche (IFR) 105, Institut d'Hématologie; and Université Paris VII Denis Diderot, Paris, France.

Submitted December 21, 2004; accepted September 19, 2005. Prepublished online as *Blood* First Edition Paper, October 4, 2005; DOI 10.1182/blood-2004-12-4856.

Supported by research grant GOA/2004/09 (Geconcerteerde Onderzoeksactie) from the University of Leuven; grant HL 68003 from the National Heart, Lung and Blood Institute of the National Institutes of Health (NIH); and a travel grant provided in cooperation by INSERM and the Ministry of the Flemish Community. During this study, A.B. was the recipient of a Marie-Curie fellowship (project QLGA-CT-2000-51165), a Marie-Curie European Reintegration Grant (project MERG-CT-2004-006377), and a grant from the Fondation pour la Recherche Médicale. K.D. was the recipient of a junior fellowship from the University Hospital of Leuven. H.B.F. is supported by Vlaams Instituut voor de Bevordering van het Wetenschappelijk-technologisch onderzoek in de Industrie (IWT) grant no. 21394.

A.B. and K.D. contributed equally to this work.

Reprints: Marc Hoylaerts, Center for Molecular and Vascular Biology, University of Leuven, Campus Gasthuisberg, Herestraat 49, B-3000 Leuven, Belgium; e-mail: marc.hoylaerts@med.kuleuven.ac.be.

The publication costs of this article were defrayed in part by page charge payment. Therefore, and solely to indicate this fact, this article is hereby marked "advertisement" in accordance with 18 U.S.C. section 1734.

recruitment of platelets to inflamed endothelium has been suggested by Lagadec et al.[15]

Following disruption of the *Tsp1* gene by homologous recombination in mice,[16] several studies have tried to elucidate the function of TSP-1 in vivo, but have not specifically addressed its role in hemostasis and thrombosis. Such studies are warranted though, since single-nucleotide polymorphisms in multiple novel thrombospondin genes may be associated with familial premature myocardial infarction.[17] In addition, persistent elevation of TSP-1 in cardiac allografts correlates with the development of cardiac allograft vasculopathy.[18] Recently, TSP-1, like ADAMTS13, was found to bind to the A3 domain of VWF, an interaction suggested to lead to competition with ADAMTS13, slowing the rate of ADAMTS13-mediated VWF proteolysis.[19]

The present analysis demonstrates a role for TSP-1 in vascular biology and underscores that soluble TSP-1–endothelium interactions enhance the dynamic recruitment of platelets to stimulated endothelial cells, in part, because TSP-1 protects endothelium-bound VWF from plasma ADAMTS13-mediated degradation. It also documents that TSP-1 secures the anchoring of a developing thrombus to damaged venules and arterioles, likewise by protecting subendothelial VWF from being cleaved by circulating ADAMTS13.

Materials and methods

Reagents

Rabbit polyclonal antibodies against human TSP-1, isolated from platelets, were raised in the laboratory; they reacted both with human and murine TSP-1 in Western blotting. Human anti-ADAMTS13 antibodies were isolated from the plasma of 4 nonrelated patients with acquired thrombotic thrombocytopenic purpura (TTP) and pooled. The VWF-neutralizing monoclonal antibody AJvW-2 was from Ajinomoto (Kawasaki, Japan). Goat anti–human IgG $F(ab')_2$ antibodies were from Biosource (Camarillo, CA) and Fc-specific goat anti–human IgG antibodies, conjugated with human horseradish peroxidase, were from Sigma (St Louis, MO). Rabbit and patient antibodies were purified by Protein-A Sepharose chromatography, and purified anti-ADAMTS13 immunoglobulins were aliquoted. Peroxidase-conjugated and nonconjugated rabbit polyclonal anti-VWF antibodies, peroxidase-conjugated goat anti–rabbit IgG antibodies, and antifibronectin and antifibrinogen polyclonal antibodies were from Dako (Glostrup, Denmark). The calcium ionophore A23187 and the nonionic detergent NP-40 (IGEPAL CA360) were from Sigma. The peptide H-Arg-Phe-Tyr-Val-Val-Met-Trp-Lys-OH (4N1K) corresponding to residues 1016-1023 of TSP-1 was from Bachem (Bubendorf, Germany); calcein-AM was purchased from Molecular Probes (Leiden, the Netherlands). Lepirudin was from Hoechst (Frankfurt, Germany) and prostaglandin PGE_1 (Prostin) was from Pharmacia (Uppsala, Sweden). Native type I collagen fibrils from equine tendon (collagen reagent Horm) were from Nycomed (Munich, Germany), and protease inhibitor cocktail Complete tablets were from Hoffman-La Roche (Basel, Switzerland).

Isolation of human platelet thrombospondin-1

Human TSP-1 was purified according to Dubernard and Legrand[20] with modifications: platelet-rich plasma (PRP) was acidified with 0.1 volume of concentrated acid-dextrose-citrate (ACD-C; 130 mM citric acid, 153 mM sodium citrate, 111 mM glucose, pH 6.5) in the presence of 100 nM PGE_1 and centrifuged at 700*g* for 20 minutes. Platelets were resuspended in wash buffer (36 mM citric acid, 5 mM glucose, 5 mM KCl, 2 mM $CaCl_2$, 1 mM $MgCl_2$, 103 mM NaCl, pH 6.5) containing 0.1 volume of ACD-C and 100 nM PGE_1. The wash step was repeated twice. Platelets were then resuspended in 1 L reaction buffer (15 mM Tris-HCl, 150 mM NaCl, 2 mM $CaCl_2$, pH 7.6) at 10^{12} platelets/L, and activated with bovine α-thrombin (0.5 U/mL; Sigma). After 2 minutes, the reaction was stopped by adding lepirudin (10 μg/mL), 2 tablets of the Complete protease inhibitor cocktail, 2 mM benzamidine, and 100 μM phenyl-methyl-sulfonyl fluoride (PMSF). From this step onward, the entire purification process was done at 4°C. The NaCl concentration was adjusted to 300 mM and degranulated platelets were cleared by centrifugation at 5000*g* for 15 minutes. After a freezing step at −20°C for 48 hours, the supernatant was centrifuged at 18 000*g* for 15 minutes to remove the cryoprecipitate and remaining cell fragments, and was passed through a heparin–Sepharose 6B column (Amersham Biosciences, Uppsala, Sweden). Bound TSP-1 was eluted with 15 mM Tris-HCl, pH 7.5, containing 550 mM NaCl, 2 mM $CaCl_2$, 100 μM PMSF, and 0.05% sodium azide. It was concentrated with Aquacide II (Calbiochem) and loaded onto a Sepharose CL-4B column (Amersham Biosciences). Eluted fractions corresponding to TSP-1 were pooled, concentrated, and dialyzed overnight against 15 mM Tris-HCl, pH 7.5, containing 300 mM NaCl and 2 mM $CaCl_2$. SDS-PAGE with Coomassie Brilliant Blue staining revealed a homogeneous TSP-1 band and Western blotting confirmed the absence of contaminating fibrinogen, VWF, and fibronectin.

Mouse platelet isolation and processing

Blood was taken on hirudin (20 μg/mL) via puncture of the caval vein of mice anesthetized with nembutal (60 mg/kg intraperitoneally). PRP was obtained by consecutive centrifugation of the blood for 30 seconds at 800*g* and 5 minutes at 150*g*. Upon addition of 0.2 volumes of acid-dextrose-citrate (ACD: 93 mM Na_3-citrate, 7 mM citric acid, 0.14 M dextrose, pH 6.5), platelets were isolated by centrifugation at 800*g* for 5 minutes.

Platelet lysate SDS-PAGE and VWF multimer agarose gel electrophoresis

Blood from 3 WT or *Tsp1*–null mice was collected in 1:10 ACD and 20 μg/mL hirudin. PRP were harvested and pooled as reported and platelets were counted. Platelets were then pelleted at 800*g*, resuspended, and lysed for 30 minutes at the same final platelet concentration in both the WT and the *Tsp1* gene-deficient pools (in approximately 1:2 of the initial PRP volume) in phosphate-buffered saline (PBS) containing 1% IGEPAL and a cocktail of protease inhibitors (Complete, dissolved at 1 tablet per 50 mL of buffer). After 3 fast liquid N_2 freezing and thawing steps, samples were centrifuged for 10 minutes at 14 000*g* and supernatants were analyzed by SDS-PAGE in reducing conditions, for TSP-1, fibronectin (Fn), and Fg or by electrophoresis in 1.4% agarose for the analysis of VWF multimers. Electrophoresis was followed by Western blotting, using monospecific antibodies for the detection of the indicated proteins.

Platelet labeling for intravital microscopy

Platelets from one mouse were resuspended at 500×10^9 platelets/L in 200 μL Tyrode buffer (12 mM $NaHCO_3$, 0.42 mM NaH_2PO_4, 137 mM NaCl, 2.7 mM KCl, 1 mM $MgCl_2$, 5 mM HEPES, 0.35% human serum albumin), incubated (15 minutes, 37°C) with 10 μg/mL calcein, and then directly injected into the circulation via the catheterized jugular vein. In some experiments, the peptide 4N1K (100 μM) was added to the platelets during the incubation with calcein, prior to injection.

Electron microscopy

Isolated platelets from 3 WT or *Tsp1*–null mice resuspended in Tyrode buffer were fixed overnight at 4°C in 2.5% (wt/vol) glutaraldehyde and 0.1 M phosphate buffer, pH 7.2. After centrifugation at 800*g* for 10 minutes, a condensed pellet of platelets was formed. After fixation in 1% OsO_4 (wt/vol) and 0.1 M phosphate buffer, pH 7.2, and dehydration in graded series of ethanol, the pellets were embedded in epoxy resin. Ultrathin sections were cut and stained with uranyl acetate and lead citrate before examination with a Zeiss EM 10 electron microscope (Oberkochen, Germany).

Antigen and activity assays

Human IgGs in plasma of mice treated with patient anti-ADAMTS13 antibodies or human control immunoglobulins were measured via enzyme-linked immunosorbent assay (ELISA), using microtiter plates coated with goat anti–human IgG $F(ab')_2$ antibody fragments, followed by detection of bound IgG with Fc-specific goat anti–human IgG, coupled to peroxidase, according to standard procedures, using human IgG as a reference.

The human TSP-1 concentration in plasma of *Tsp1*$^{-/-}$ mice treated with a bolus of human TSP-1 of 80 μg/kg plus infusion of 80 μg/kg/h for 30 minutes, was determined in microtiter plates coated with a homemade monoclonal antibody (36A8, equally reactive with human and murine TSP-1), followed by detection of bound TSP-1 by biotinylated rabbit anti–TSP-1 antibodies, according to classical procedures. Reference curves of human TSP-1 were constructed in 20-fold diluted *Tsp1*$^{-/-}$ plasma, and experimental samples were measured in 20-fold diluted mouse plasma, yielding very low background signals.

Inhibitory properties of purified anti-ADAMTS13 antibodies were measured in an ADAMTS13 activation assay, in the presence of urea as described,[21] upon inclusion of the purified antibodies (0-1 mg/mL). Protease activity neutralization was assessed via VWF multimer agarose electrophoresis, as described or via a VWF-collagen binding ELISA.[21]

Recombinant ADAMTS13 production and isolation

ADAMTS13 was expressed as a fusion protein, containing a C-terminal 6 × His tag and V5 recognition epitope. The inducible GeneSwitch mammalian expression system was used, according to the instructions of the manufacturer (Invitrogen, Carlsbad, CA). In brief, ADAMTS13 cDNA was cloned in the pGene expression vector (Invitrogen) and stably transfected in a CHO cell line. When confluency was reached, medium was supplemented with 100 nM steroid inductor (mifepristone) and incubated for 72 hours. Expression medium was concentrated 7-fold by ultrafiltration and purified by Ni-chelating chromatography on a HisTrap column according to the instructions of the supplier (Amersham Biosciences, Freiburg, Germany).

In vitro perfusion of human calcein-labeled platelets

In vitro perfusion of calcein-labeled platelets, resuspended in reconstituted blood at 20×10^9 platelets/L over layers of confluent EA.hy926 endothelial cells, was done as reported before, with constant monitoring of platelet–endothelial cell interactions via online videomicroscopy.[22,23] When indicated, endothelial cells were preperfused with A23187 (50 μM; dissolved in HEPES-Tyrode buffer, containing 1 mM $CaCl_2$ and 1 mM $MgCl_2$) for 6 minutes, followed by a washout for 5 minutes with the same buffer, without $MgCl_2$ or $CaCl_2$. The perfusion flow rate was 1.5 mL/min, corresponding to a shear rate of 600 s^{-1}. Plasma was added to the reconstituted blood at a ratio of 3 mL to 8 mL final volume.

To measure the cleavage of ultralarge VWF multimers by recombinant ADAMTS13, the A23187-preperfused endothelial cells were washed for 5 minutes with HEPES-Tyrode buffer and then superfused with calcein-labeled platelets at 20×10^9 platelets/L resuspended in reconstituted blood, for 10 minutes, followed by a washout for 3 minutes with buffer, before recombinant ADAMTS13 (with or without added TSP-1 at 3 μg/mL, or control buffer) was perfused for 10 minutes, and dissolved in reconstituted blood to 2 nM further containing 20 μM Zn-acetate (in the absence of platelets and without $MgCl_2$ or $CaCl_2$). At the end of this perfusion, the number of waving platelet strings was counted in 10 unrelated microscopic fields, to measure those VWF multimers long enough to carry platelets and stick out in the perfusate.

Animal models

Tsp1 gene–deficient mice. *Tsp1*–null mice in which the *Tsp1* gene was disrupted by homologous recombination have previously been described.[16] For this study, the *Tsp1* gene deficiency was bred into a Swiss background (98.4%) to enable in vivo analysis of thrombosis. All animal experiments were reviewed and approved by the Institutional Review Board of the University of Leuven, and were performed in compliance with the guidelines of the International Society on Thrombosis and Haemostasis.[24]

Lethal pulmonary thromboembolism model. Thromboembolism was induced by injection of a mixture of collagen (1 mg/kg) and epinephrine (120 μg/kg) into the jugular vein of mice (10 to 16 weeks old) anesthetized with nembutal. Mice breathing beyond 20 minutes after injection were considered to be survivors.[25]

Localized stimulation of the endothelium by A23187. A model simulating locally inflamed blood vessels was used, adapted from André et al.[26] WT or *Tsp1*–null Swiss mice (4 to 5 weeks old) were anesthetized with nembutal, the jugular vein was catheterized, and calcein-labeled platelets were injected via the catheter. After 10 minutes, during which circulating platelets reached a steady state, the mesentery was externalized and mesenteric venules were exposed on the table of the epifluorescence microscope. A23187 calcium ionophore, a known secretagog of Weibel-Palade bodies, then was superfused (10 μL at 30 μM) on a venule and platelet recruitment was studied as follows. Recording of movies (10 minutes with 1 frame taken every 3 seconds) was started 30 seconds before the onset of the superfusion. When indicated, a bolus plus infusion of purified human TSP-1 or of anti-ADAMTS13 antibodies were administered to the mice via the catheterized jugular vein, with infusion lasting for 1 hour and started just prior to endothelium activation. The following parameters were analyzed over a 10-minute interval: number of labeled platelets accumulating on the activated endothelium of mesenteric blood venules at 1-minute intervals, up to 10 minutes; and percentage of vessels exhibiting platelet tethering (stop-and-go motion), platelet firm adhesion (static adhesion with no detachment and a fast decrease of the platelet fluorescence, indicative of platelet release due to activation), and the formation/disappearance of platelet strings.

Photochemically induced thrombosis (PIT). WT or *Tsp1*-null mice (10 to 16 weeks old) were anesthetized with nembutal via intraperitoneal injection, and the jugular vein was catheterized. Mice were positioned on the table of an inverted epifluorescence microscope (Diaphot; Nikon, Melville, NY) and the intestines were exposed such that the arterioles and venules covering the cecum were visualized through a Cohu CCD video camera (Cohu, San Diego, CA). Fluorescently labeled murine platelets were then injected through the catheterized jugular vein (10^{12} platelets/L in 200 μL). Following IV injection of rose-bengal (10 mg/kg bolus followed by IV infusion at 10 mg/kg/h for 40 minutes following injury), selected arterioles/venules were exposed for 20 seconds to green light, focused via the microscope objective, resulting in localized and reproducible vessel wall injury over a distance of about 500 μm. When indicated, a bolus plus infusion of purified human TSP-1 and/or lepirudin or of anti-ADAMTS13 antibodies were administered to mice via the catheterized jugular vein, with infusion lasting for 1 hour and started just prior to injury induction. The recruitment of labeled platelets to the lesion site (adhesion and aggregation) was observed in real time, digitized with a Scion LG3 frame grabber (Scion, Frederick, MD) and recorded in the memory of an attached computer for later analysis with the NIH Image program version 6.1. Two parameters were analyzed: the vessel occlusion time, defined as blood flow arrest for at least 1 minute; and the number of massive emboli, a massive embolus being defined as the detachment and transport of an entire occluding thrombus.

The anticoagulant effect of the administered lepirudin was measured ex vivo in citrate plasma taken from separate lepirudin-treated mice via thrombin generation curves constructed in a Thrombinoscope[27] upon addition of 1 pM recombinant human tissue factor (Innovin, Dade Behring, Liederbach, Germany) to reference mouse plasma or to lepirudin-containing plasma. Peak thrombin concentrations generated in recalcified plasma were reduced from 40 nM in control plasma to concentrations ranging from 4 to 10 nM, (mean, 7 ± 3 nM; n = 4) in lepirudin-containing plasmas, isolated from separate mice (not shown).

Statistics

The statistical significance between means was assessed via nonparametric tests, with correction, when indicated in the legends of the figures. Two-tailed *P* values were calculated. Also, 2 × 2 contingency table

analyses were performed with a Fisher exact test to compare different distribution of data in the different treatment or gene-deficient groups.

Results

Tsp1$^{-/-}$ mouse platelet morphology

Electron microscopy revealed that the shape, size, and overall morphology of resting mouse platelets were not affected by the absence of TSP-1 in the platelet α-granules (Figure 1). Despite absent TSP-1, abundantly present in WT platelets, the number and distribution of platelet dense and α-granules were similar in *Tsp1*$^{-/-}$ platelets (Figure 1). The α-granule contents of Fn, Fg, and VWF, other adhesive molecules known to be involved in platelet adhesion and aggregation, were not different between *Tsp1*–null and control platelets when analyzed via Western blotting of platelet lysates. In contrast to recent findings obtained in *Tsp1*$^{-/-}$ mice bred into C57BL/6 mice,[19] the VWF multimer size distribution patterns in platelet and plasma VWF pools were identical, a conclusion supported by density scans of the corresponding lanes (Figure 1). Injection of human TSP-1 in the circulation of mice did not induce VWF size differences in WT or *Tsp1*$^{-/-}$ plasma derived from the corresponding Swiss mice in the present study (not shown) when measured 24 hours later.

Tsp1$^{-/-}$ platelet aggregation is not impaired in vitro

Tsp1–null platelets were previously shown to respond normally to various concentrations of thrombin when stirred in the cuvette of an aggregometer.[16] In this study, we further tested the response of *Tsp1*–null platelets to other platelet agonists. The aggregation responses in PRP from WT and *Tsp1*–null mice were equivalent when triggered by ADP (2, 5, or 10 μM), the TxA_2 analog U46619 (1.5 to 5 μM), or native type I collagen fibrils from equine tendon (0.3 or 0.5 μg/mL) (data not shown).

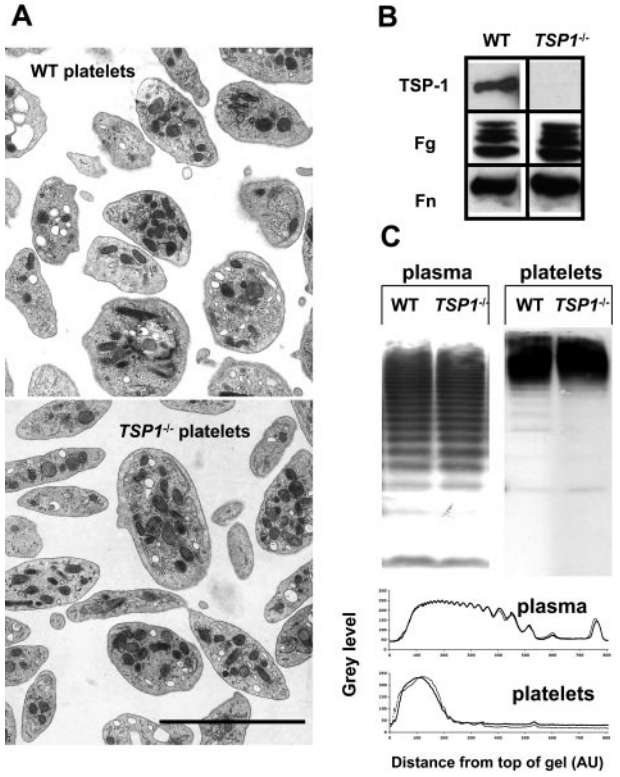

Figure 1. General morphology and composition of *Tsp1*–null platelets. (A) Transmission electron microscopy of murine WT platelets and *Tsp1*$^{-/-}$ platelets. The scale bar represents 5 μm. (B) SDS-PAGE under reducing conditions and Western blot analysis of the platelet content in TSP-1, fibrinogen (Fg), and fibronectin (Fn), as indicated. (C) Multimer analysis via agarose gel electrophoresis of von Willebrand factor (VWF) in WT and *Tsp1*$^{-/-}$ plasma and platelets, with representative scans of the multimer distribution patterns. AU indicates arbitrary units.

Table 1. Rheologic characteristics of venules and arterioles of WT and *Tsp1*-null mice

Genotype mice and vessel type	Diameter, μm	Shear rate, s^{-1}
WT		
Mesenteric venules	172.3 ± 5.5	173.2 ± 22.6
Caecum venules	105 ± 32	337.3 ± 17.3
Caecum arterioles	52 ± 23*	662.0 ± 87.2
Tsp1-null		
Mesenteric venules	195.2 ± 6.1	168.5 ± 15.1
Caecum venules	109 ± 27	289.1 ± 21.3
Caecum arterioles	68 ± 16*	652.5 ± 58.9

Values are mean ± SEM. The platelet count for WT mice was 666 ± 95 × 10^9/L and hematocrit was 32% ± 3%; for *Tsp1*-null mice, the platelet count was 664 ± 174 × 10^9/L and hematocrit was 33% ± 4%.

*P = .01.

Platelet recruitment onto stimulated endothelium is impaired in *Tsp1*$^{-/-}$ mice

Treatment of blood vessels with the calcium ionophore A23187 stimulates endothelium and triggers degranulation of endothelial Weibel-Palade bodies, thus inducing immediate platelet tethering and also firm adhesion to the endothelium, largely caused by VWF multimers retained on the endothelium.[23,26] To investigate in vivo whether TSP-1 is instrumental in the interaction between circulating platelets and stimulated endothelium, in a first approach, we stimulated mesenteric venules of WT or *Tsp1*–null mice via local superfusion with A23187, and followed the interaction between flowing calcein-labeled platelets and endothelium in real time. The wall shear rate (approximately 170 s^{-1} estimated from the velocity of free fluorescently labeled injected platelets flowing in the center of the vessels) and the diameter of the venules studied (about 180 μm) were similar in both genotypes (Table 1).

After initiation of endothelial cell degranulation, the time at which tethering could be first observed (time-to-tethering in Figure 2A) was considerably shorter in WT mesenteric vessels than in *Tsp1*$^{-/-}$ vessels. In a large fraction of the *Tsp1*$^{-/-}$ vessels, no tethering was observed within 200 seconds upon *Tsp1*$^{-/-}$ platelet injection and a wider time-to-tethering distribution was apparent in the *Tsp1*–null mice than in WT mouse blood vessels. Reconstitution of *Tsp1*–null mice with purified human TSP-1 (bolus of 80 μg/kg + infusion of 80 μg/kg/h) or pretreatment of the injected *Tsp1*$^{-/-}$ platelets with the CD47-activating peptide 4N1K partially restored the time-to-tethering to a mean value about half of that for nontreated *Tsp1*$^{-/-}$ mice, although still higher than measured for WT platelets (Figure 2A). More detailed counts of the number of mesenteric venules showing tethering and firm adhesion of injected platelets respectively, revealed considerably weaker endothelium-platelet interactions in *Tsp1*–null mice than in WTs (Figure 2B). Crossover experiments (Figure 2B) revealed both a lower tethering and adhesion when WT platelets were injected in *Tsp1*–null mice than for *Tsp1*$^{-/-}$ platelets injected in WT mice, the latter response being normal. These experiments provide evidence for a major contribution of soluble and endothelium-associated TSP-1 in platelet recruitment on stimulated endothelium, rather than of platelet TSP-1. Soluble TSP-1 injection indeed restored both tethering and firm adhesion in *Tsp1*$^{-/-}$ mice that received injections

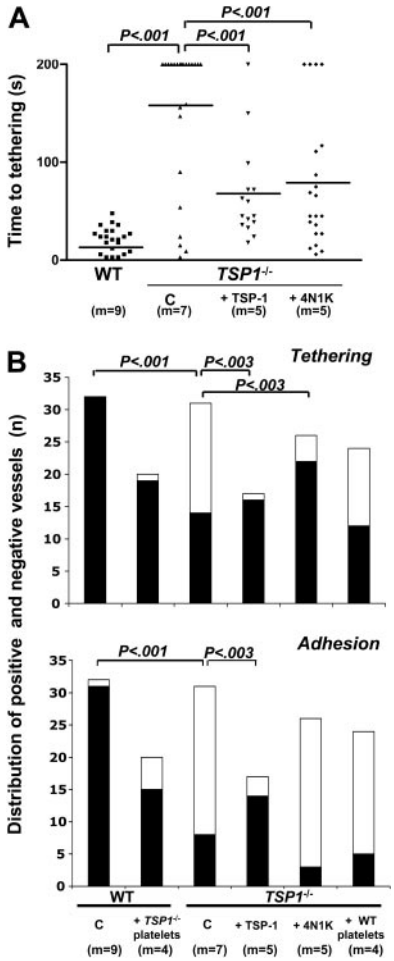

Figure 2. Platelet recruitment on A23187-stimulated endothelium in vivo. (A) Dot plot representation of the time in seconds (s) until initiation of platelet tethering in vivo on endothelium of murine mesenteric venules stimulated with A23187 for the indicated number of mice (m). Means are represented as short horizontal lines; indicated 2-tailed *P* values were calculated by unpaired nonparametric Mann-Whitney test with Welch correction for nonequal variances. (B) Distribution of numbers of mesenteric vessels, reactive (■) and nonreactive (□) with platelets, during analysis of tethering and firm adhesion, as indicated for the mentioned number of mice (m); indicated *P* values were calculated by 2 × 2 contingency table analysis and Fisher exact test with 2-sided *P* value. C indicates nontreated controls; +TSP-1, bolus of 80 μg/kg + infusion of 80 μg/kg/h; +4N1K, injection with calcein-labeled platelets preactivated with 100 μM of the CD47 activating peptide 4N1K; and +*Tsp1*$^{-/-}$ platelets and +WT platelets, cross-design experiments with platelet injection in WT and *Tsp1*$^{-/-}$ mice, respectively.

of *Tsp1*$^{-/-}$ platelets. Interestingly, 4N1K pretreatment of platelets restored platelet tethering, but not firm adhesion (Figure 2B), pointing to a role for TSP-1 in the control of integrin activation via IAP (CD47), but uncovering a ligand function for TSP-1, required for firm platelet adhesion to the endothelium in addition to receptor activation, the latter being mimicked by 4N1K. In the absence of platelet activation, TSP-1 stored within platelet α-granules is inactive.

TSP-1 binding to endothelium has been reported before[15] and is substantiated by the finding that after administration of bolus plus infusion of human TSP-1, the mean plasma TSP-1 concentration in *Tsp1*$^{-/-}$ mice reached 126 ± 71 ng/mL, instead of the anticipated 1000 ng/mL, based on a rodent distribution volume of 80 mL/kg.

Because platelet-vessel wall interactions between WT and *Tsp1*$^{-/-}$ mice differed mostly with regard to platelet adhesion, more detailed kinetic measurements were made of the firm adhesion of platelets on A23187-activated mesenteric blood vessels over an interval of 10 minutes. Figure 3 confirms substantial differences in the degree of gradual platelet accumulation for WT and *Tsp1*$^{-/-}$ mice. Pretreatment of *Tsp1*$^{-/-}$ mice with human TSP-1 (80 μg/kg + 80 μg/kg/h) raised platelet recruitment in *Tsp1*$^{-/-}$ mice to values even slightly higher than in nontreated WT mice (Figure 3). Correspondingly, administration of TSP-1 to WT mice could further elevate platelet adhesion to similar values (Figure 3). Platelet adhesion in *Tsp1*$^{-/-}$ mice could also be restored by administration of neutralizing anti-ADAMTS13 antibodies (23 mg/kg + 23 mg/kg/h) derived from TTP patients (Figure 3, bottom) to a similar degree as with TSP-1, such antibodies also having an effect in WT mice comparable with that of TSP-1. Plasma levels for this antibody, measured 30 minutes after the start of the infusion, reached 152 ± 49 μg/mL, compared with the target of 280 μg/mL. An in vitro inhibition assay of VWF degradation by ADAMTS13 in urea confirmed that these antibodies inhibited protease activity, yielding 50% inhibition at 400 μg/mL in this nonphysiologic assay (not shown). In contrast, administration of irrelevant human immunoglobulins to a plasma concentration of 418 μg/mL did not trigger TSP-1$^{-/-}$ platelet adhesion in TSP-1–null mice (Figure 3).

TSP-1 modulates ADAMTS13-controlled platelet string formation

Perfusion of endothelial cells with calcein-labeled platelets in reconstituted blood (without plasma) in vitro resulted in firm platelet adhesion as reported[28,29] and as illustrated in Figure 4. Endothelial cell stimulation with A23187 increased the subsequent firm platelet adhesion several-fold (Figure 4B). In addition, A23187 stimulation resulted in adhesion of platelets to ultralarge VWF

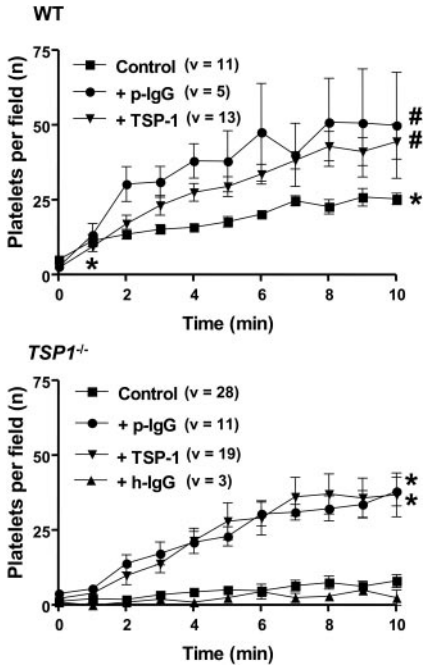

Figure 3. Kinetics of platelet adhesion on A23187-stimulated mesenteric blood vessels. Mean number (± SEM) of firmly adhering platelets after start of A23187 stimulation of mesenteric endothelium as a function of time upon injection with homologous calcein-labeled platelets in WT (WT) and *Tsp1*–null mice (*Tsp1*$^{-/-}$) in nontreated controls (Control) and in mice treated with irrelevant human IgG (23 mg/kg + 23 mg/kg/h; h-IgG), anti-ADAMTS13 IgG (23 mg/kg + 23 mg/kg/h; p-IgG), and human TSP-1 (80 μg/kg + 80 μg/kg/h); number of mice varied from 1 (h-IgG treatment) to 5 (*Tsp1*–treated TSP-1–null mice); v indicates number of vessels analyzed; *P* values were calculated via nonparametric Mann-Whitney test, with 2-tailed P-value (*$P < .001$ vs *Tsp1*$^{-/-}$ Control analyzed at minutes 1 and 10, respectively; #$P < .05$ vs WT Control, analyzed at minute 10).

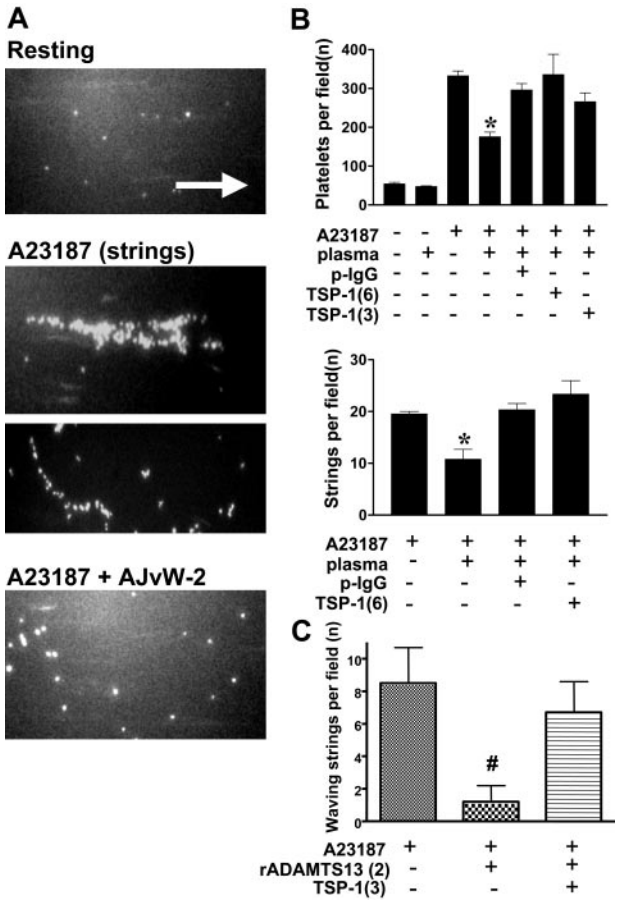

Figure 4. Platelet string formation on stimulated human endothelial cells. Platelet adhesion to resting and A23187 (30 μM)–stimulated human EA.hy926 endothelial cells during perfusion of calcein-labeled human platelets (20×10^9 platelets/L) in reconstituted blood. (A) Platelet strings form on A23187-stimulated endothelial cells; they are prevented in the presence of the VWF-neutralizing antibody AJvW-2. Objective, 10×/long working distance numerical aperture (B) Mean numbers (± SEM) of platelets adhering per field and of strings formed, before and after endothelial cell stimulation, followed by perfusion with reconstituted blood, supplemented with human plasma, containing anti-ADAMTS13 antibodies (p-IgG; 250 μg/mL) or human TSP-1 at 6 or 3 μg/mL, as indicated. (C) Mean numbers (± SD) of waving strings formed per field after endothelial cell stimulation, followed by perfusion with reconstituted blood containing calcein-labeled human platelets (20×10^9 platelets/L) and subsequent perfusion with human recombinant ADAMTS13 (2 nM) supplemented with human TSP-1 at 3 μg/mL, as indicated. The white arrow (length = 50 μm) represents the direction of the blood flow (*$P < .01$; #$P < .001$ vs A23187 stimulation).

multimers anchored to the endothelial surface, forming strings of platelets (Figure 4A). Strings disappeared in the presence of the VWF-neutralizing antibody AJvW-2, confirming the role of ultra-large VWF multimers in platelet recruitment. Inclusion of normal human plasma in the perfusate reduced the total platelet adherence considerably, a defect largely corrected when the plasma was supplemented with TSP-1 or anti-ADAMTS13 antibodies (Figure 4B). The same trend was found when the total number of strings in each microscopic field was counted; these results show that in a more physiologic assay than the urea-based ADAMTS13 assay, 250 μg/mL anti-ADAMTS13 antibodies are capable of neutralizing plasma ADAMTS13. During additional platelet perfusions over coated human TSP-1 in the presence of soluble VWF added to physiological concentrations, the deposition of platelets was reduced by VWF, at all shear rates investigated (not shown). These findings therefore suggest that the correction by TSP-1 in Figure 4B resulted from an indirect contribution of TSP-1 to platelet recruitment via VWF, rather than from cross-bridging TSP-1–VWF interactions (see "Discussion").

Finally, perfusions over A23187-stimulated endothelial cells with calcein-labeled platelets and subsequent shear stress–controlled perfusions with recombinant ADAMTS13 revealed that the number of long, waving platelet strings was reduced from 8.5 to 1.2 per field (Figure 4C). The presence of TSP-1 in the second perfusate largely prevented the breakdown of long, waving strings by recombinant ADAMTS13 (6.7 per field). Hence, these findings show that about half the strings formed upon perfusion of platelets over A23187-stimulated endothelium are mobile and subject to a functionally detectable size control by ADAMTS13, a process largely inhibited by TSP-1.

Similarly to the in vitro perfusions of platelets over activated endothelial cells, only a few seconds after the start of the mesenteric WT venule perfusion with A23187, strings of 4 to 7, and up to 10 calcein-labeled platelets were visible on the vessel wall, in the direction of flow (Figure 5A-C). Most strings detached within 3 seconds, but occasionally adhered longer and disappeared progressively, starting from the head of the string (ie, its upstream extremity), as illustrated for one string, and gradually being shortened over a time interval of 15 seconds (Figure 5D). The percentage of mesenteric venules exhibiting platelet strings upon endothelial stimulation by A23187 was higher in WT than in *Tsp1*$^{-/-}$ mice (48% versus 20%: $P < .04$; Figure 5E). Interestingly, TSP-1 (80 μg/kg + 80 μg/kg/h) raised this percentage in TSP-1–null mice to 75% ($P < .001$ vs *Tsp1*-null mice), seemingly higher than in WT mice, and in further agreement with the analysis of firm platelet adhesion (Figure 3). In contrast, pretreatment of calcein-labeled *Tsp1*$^{-/-}$ platelets with 100 μM 4N1K prior to injection did

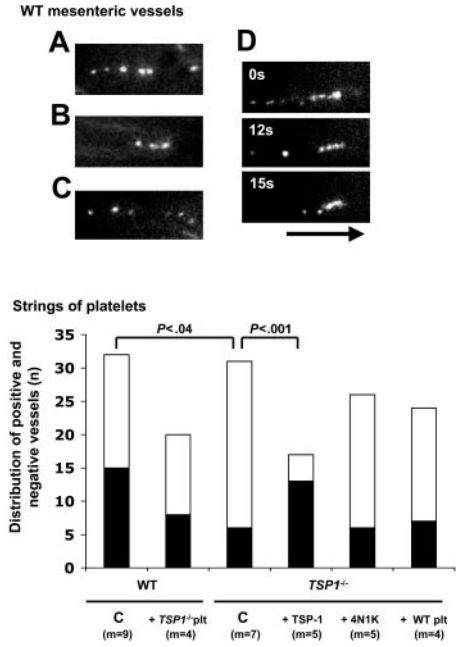

Figure 5. Platelet string formation on stimulated murine endothelium. (A-C) Individual examples of strings of adherent platelets on endothelium of exposed mesenteric venules following stimulation with exogenously administered A23187. (D) Example of progressive string resorption over an interval of 15 seconds. The black arrow (length = 50 μm) represents the direction of the blood flow. (E) Distribution of numbers of mesenteric vessels, demonstrating platelet string formation (■) or not (□), following vessel stimulation by A23187, for the indicated number of mice (m); indicated *P* values were calculated by 2 × 2 contingency table analysis and Fisher exact test with 2-tailed *P* value. C indicates nontreated controls; +TSP-1, bolus of 80 μg/kg + infusion of 80 μg/kg/h; +4N1K, injection with calcein-labeled platelets preactivated with 100 μM of the CD47-activating peptide 4N1K; and +*Tsp1*$^{-/-}$ platelets and +WT platelets, cross-design experiments with platelet injection in WT and TSP-1$^{-/-}$ mice, respectively.

not significantly alter the percentage of strings formed by these platelets in venules of *Tsp1*-null mice (25%; $P = .74$). Crossover design experiments (WT platelets in *Tsp1*-null mice versus the opposite) did not affect the degree of string formation (Figure 5). These experiments confirmed that TSP-1 corrects an adhesive phenotype, different from integrin activation controlled via 4N1K.

TSP-1 in pulmonary thromboembolism

Because TSP-1 plays a role in the early activation of platelets upon adhesion to collagen,[12] we first examined the consequences of TSP-1 deficiency in a model of lethal thromboembolism induced by injection of native type I collagen fibrils from equine tendon (1 mg/kg) in combination with epinephrine (120 μg/kg). In this model of potent in vivo aggregation of circulating platelets and occlusion of the pulmonary circulation by aggregates, survival frequencies 20 minutes after injection were not significantly different between the WT (40%, n = 10) and *Tsp1*-null mice (37.5%, n = 8) ($P > .999$), in agreement with the in vitro platelet aggregation data (not shown), revealing identical platelet activations. The mean survival time in the *Tsp1*-null mice (206 ± 22 seconds, n = 7) appeared slightly shorter than in WT controls (290 ± 41 seconds, n = 6; 2-tailed $P < .003$, by unpaired *t* test, with Welch correction).

Impaired thrombus adherence in TSP-1–null mice

Since TSP-1 increased the VWF-dependent platelet adhesion to stimulated endothelium, we then investigated the role of TSP-1 in the VWF-dependent thrombus development in venules and arterioles of the cecum after endothelial injury. Table 1 shows that the relevant hematologic and rheologic parameters in WT and *Tsp1*$^{-/-}$ mice were comparable, but that arterioles in the cecum slightly differ in diameter between the 2 genotypes. In WT mice, upon photochemical injury, thrombi progressively developed in injured blood vessels, until complete occlusion occurred at a mean of 9.3 ± 1 minutes in venules and 12.2 ± 3 minutes in arterioles. The distribution of occlusion times (Figure 6) was larger in arterioles than in venules; mean values were roughly doubled in *Tsp1*$^{-/-}$ mice, both for the occlusion of arterioles (23.7 ± 1.7 minutes) and venules (17.6 ± 1.3 minutes). TSP-1 (80 mg/kg + 80 μg/kg/h) restored normal vessel occlusion in *Tsp1*–null mice (mean occlusion times of 8.1 ± 1.3 minutes in venules and 7.9 ± 1.9 minutes in arterioles (Figure 6). Likewise, the anti-ADAMTS13 antibodies (23 mg/kg + 23 mg/kg/h) restored normal occlusion in *Tsp1*-null mice (mean occlusion times of 10.5 ± 1.8 minutes in venules and 10.6 ± 2.9 minutes in arterioles). Parallel administrations of TSP-1 (80 μg/kg + 80 μg/kg/h) and anti-ADAMTS13 antibodies (23 mg/kg + 23 mg/kg/h) in WT controls revealed no significant effect on the mean occlusion times, neither in venules nor in arterioles (Figure 6).

The treatment of *Tsp1*-null mice by 4N1K (4 μMole/kg + 4 μMole/kg/h) had no effect on the kinetics of thrombus formation or on the occlusion time distribution values (not shown), confirming that the normalization by TSP-1 resulted from restoration of adhesive behavior and not from a restoration of TSP-1–mediated cell signaling via IAP regulation of $\alpha_{IIb}\beta_3$ or $\alpha_2\beta_1$ activity. Moreover, close inspection of the thrombotic process revealed that prolonged occlusion times in *Tsp1*$^{-/-}$ mice did not result from defective thrombus formation but from enhanced embolization rates of already developed large thrombi. This is illustrated in Figure 7A for 2 different massive thrombi, which detach integrally as one massive embolus between 710 and 720 seconds and 800 to 810 seconds in the examples shown. A mean of 1.8 emboli occurred

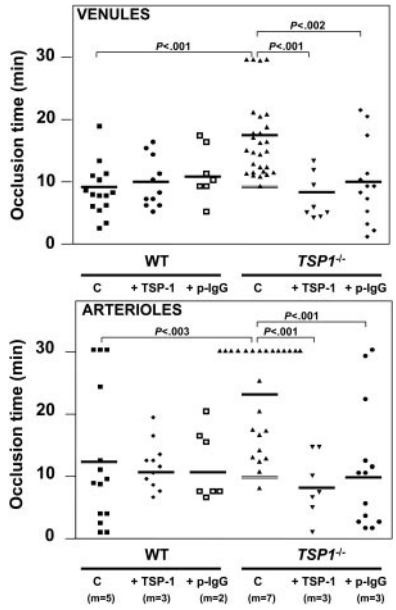

Figure 6. Photochemically injured intestinal vessel thrombosis. Distribution of occlusion time and mean (horizontal bars) upon injury induction in venules (top panel) and arterioles (bottom panel) of WT and *Tsp1*-null mice, without (*Tsp1*$^{-/-}$) or after pretreatment with human TSP-1 or anti-ADAMTS13 IgGs for the indicated number of mice (m); thin parallel lines reflect the time to first massive thrombus formation in *Tsp1*-null mice; C indicates nontreated controls; +TSP-1, bolus of 80 μg/kg + infusion of 80 μg/kg/h; and +p-IgG, bolus of anti-ADAMTS13 IgG of 23 mg/kg + infusion of 23 mg/kg/h. *P* values were calculated via nonparametric Mann-Whitney test with 2-tailed *P* value.

in *Tsp1*$^{-/-}$ cecum venules before stable occlusion; in the more narrow arterioles a similar trend could be seen, but the difference did not reach statistical significance (Figure 7B). Correspondingly, when the times to first formation of a massive thrombus (Figure 6) in the venules (8.8 ± 0.8 minutes) and in the arterioles (10 ± 1 minutes) were compared with the corresponding occlusion times in the WT blood vessels, the TSP-1 deficiency did not seem to affect the kinetics or intensity of thrombus formation per se, but caused defective thrombus adherence to the injured blood vessel. In addition, the treatment by anti-ADAMTS13 antibodies also abolished embolization, providing an explanation for the observed effects with TSP-1 (see "Discussion").

Photochemically injured thrombosis was also studied after prior administration of hirudin to mice (1.6 mg/kg + 1.6 mg/kg/h), a regimen resulting in anticoagulant effects when measured ex vivo via thrombin generation assays in mouse plasma (see "Materials and methods"). The presence of hirudin did not affect initial platelet rolling and adhesion to injured blood vessel subendothelium, but the overall cohesion of developing thrombi was reduced with more loosely organized thrombi, easily fragmenting both in WT and in *Tsp1*-null vessels (ie, resulting in retarded closure times of 12.6 ± 1 minutes and 16.8 ± 2.5 minutes in WT venules and arterioles, respectively [Figure 8]). In *Tsp1*$^{-/-}$ mice, longer occlusion times were found in venules (19 ± 1.7 minutes) and arterioles (26.3 ± 2.1 minutes). These experiments excluded implication of thrombin and fibrin formation[30] in the functional role of TSP-1 in thrombosis. Administration to hirudin-treated *Tsp1*-null mice (Figure 8) of higher concentrations of TSP-1 than applied in Figure 6 (ie, 240 μg/kg + 240 μg/kg/h and 2400 μg/kg + 2400 μg/kg/h) strongly reduced occlusion times in venules to 7.3 ± 1.1 minutes at 240 μg/kg and to 5 ± 0.5 minutes at 2400 μg/kg. Likewise, in arterioles, occlusion times were shortened to 5.1 ± 1.1 minutes and

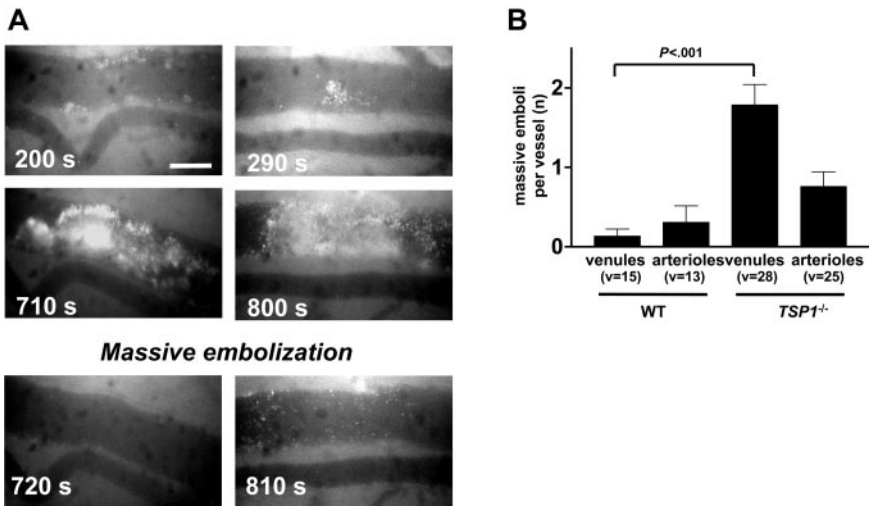

Figure 7. Embolization of *Tsp1*$^{-/-}$ platelet thrombi. (A) Examples of thrombus formation and sudden embolization (as indicated by the time in seconds) of large thrombi after intestinal venule damage in *Tsp1*-null mice. Scale bars represent 50 μm. (B) Mean number (± SEM) of embolization cycli before occurrence of occlusion in venules and arterioles of WT and *Tsp1*-null mice for the number of vessels indicated (v). *P* values were calculated via nonparametric Mann-Whitney test, with 2-tailed *P* value (*$P < .001$ between mean number of embolizations in WT and TSP-1–null mice).

4.6 ± 1.5 minutes, respectively, resulting in values even considerably shorter than in WT mice (Figure 8). These experiments confirm that the adhesive role of TSP-1 can be restored in the absence of blood coagulation.

Discussion

Thrombospondin-1 interacts with a large number of receptors involved in cellular adhesion processes, such as CD36,[31] the integrins $\alpha_{IIb}\beta_3$[32] and $\alpha_v\beta_3$,[33] proteoglycans, and the integrin-associated protein IAP (CD47)[34]; with adhesive proteins such as collagens, fibronectin and laminin, with TGF-β; and with proteases such as thrombin, elastase, and plasmin.[35] Because of its presence in the extracellular matrix of endothelial cells and in platelet α-granules, where TSP-1 constitutes one-third of the stored proteins, the role of TSP-1 in platelet aggregation has already been investigated in vitro.[36-38] Via binding to fibrinogen, itself bound to $\alpha_{IIb}\beta_3$,[10] TSP-1 enhances $\alpha_{IIb}\beta_3$ activation in association with IAP.[11] Yet, no definite hemostatic function had been ascribed to TSP-1, since TSP-1 gene-deficient mice do not manifest obvious hemostatic anomalies. TSP-1 in mice seems to be involved in the control of circulating white blood cell numbers and in persistent multiorgan inflammation,[16] and to be a potent regulator of angiogenesis.[39,40] Therefore, we presently undertook the study of TSP-1 in hemostasis, a work revealing that the in vivo role of TSP-1 in the mouse does not match the in vitro predictions,[9,41,42] although nevertheless being involved in controlling platelet adhesion to (sub)endothelium.

Standard platelet aggregation assays induced by various agonists in vitro were not different for WT and *Tsp1*$^{-/-}$ platelets, despite extensive evidence for a role for TSP-1 in platelet aggregation.[9,38,42] Although the mean survival in *Tsp1*$^{-/-}$ mice was slightly shorter than in WT mice (potentially related to the persistent pulmonary inflammation in these mice[16]), the in vivo equivalent of standard platelet aggregation tests (ie, the pulmonary thromboembolism model) did not reveal differences either, essentially demonstrating that in suspension, (collagen-induced) platelet aggregation does not require TSP-1, in vitro or in vivo. Detailed studies in a more adequate thrombosis model in arterioles and venules of the mouse likewise revealed that the time to form a primary mural thrombus did not differ in WT and *Tsp1*-null mice. These findings explicitly illustrate that at physiologic platelet numbers and physiologic plasma fibrinogen concentrations, platelet aggregate formation does not depend on the presence of TSP-1 in platelets. However, whereas in WT mouse blood vessels embolization was hardly observed, massive thrombus embolization was a frequent event in injured *Tsp1*-null vessels. Thus, our findings substantiated an important role for TSP-1 in thrombus anchorage to the vessel wall.

Defective thrombus adhesiveness to injured blood vessels in *Tsp1*–null mice could be corrected by soluble TSP-1 but not by the TSP-1–derived peptide 4N1K. Therefore, although we found that 4N1K could boost the tethering of platelets to activated endothelium, probably via CD47-mediated activation of integrin $\alpha_{IIb}\beta_3$,[11,13,15] the role of TSP-1 in firm platelet adhesion to

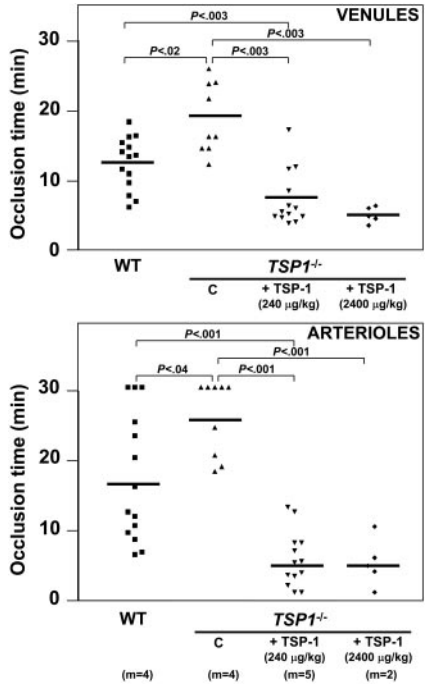

Figure 8. Intestinal vessel thrombosis during hirudin treatment. Distribution of occlusion time and mean (horizontal bars) upon injury induction in venules (top panel) and arterioles (bottom panel) of WT or *Tsp1*-null hirudin-treated mice, for the indicated number of mice (m), in control conditions (C), and after treatment with human TSP-1, either with a bolus of 240 μg/kg + infusion of 240 μg/kg/h or 2400 μg/kg + infusion of 2400 μg/kg/h; *P* values were calculated via nonparametric Mann-Whitney test, with 2-tailed *P* value.

endothelium and in thrombus stabilization onto subendothelium is different from integrin activity regulation. Firm platelet adhesion to endothelium and thrombus anchoring in *Tsp1*-null mice could also be corrected by neutralizing anti-ADAMTS13 antibodies, which are isolated from patients with an acquired form of TTP. Corresponding concentrations of TSP-1 and anti-ADAMTS13 antibodies had no measurable effect on thrombosis in WT mice, but did moderately and comparably stimulate the firm platelet adhesion to stimulated WT mouse endothelium.

In vitro perfusion studies over surfaces of (stimulated) endothelial cells clarified that TSP-1 and anti-ADAMTS13 antibodies control the same phenomenon (ie, the degradation of VWF) by the von Willebrand factor–cleaving enzyme ADAMTS13, present in plasma. This interpretation was confirmed in perfusion studies in which flexible platelet string formation was studied as a parameter to analyze VWF cleavage by recombinant ADAMTS13, a cleavage equally inhibited by TSP-1, at 3 μg/mL. Thus, our analysis illustrates that ultralarge VWF multimers are released from activated endothelial cells, confirming recent findings,[28,29] possibly, but not exclusively, involving endothelial P-selectin to temporarily retain VWF on the endothelium.[43] In response to wall shear stress, these ultralarge multimers stretch, enabling proteolysis of the VWF A2 domain by circulating ADAMTS13,[44] a physiologic process believed to contribute to the control of the size of circulating VWF multimers. However, this conclusion is inferred from the pathophysiologic accumulation of ultralarge VWF multimers in patients with TTP, deficient in ADAMTS13 activity.[45] On the other hand, VWF is released from endothelial cells as the result both of constitutive secretion, and after Weibel-Palade release, both processes differentially regulated.[46] Furthermore, it is becoming increasingly clear that environmental factor and modifier genes also contribute to the manifestation of TTP, with all these factors potentially determining the plasma VWF multimer distribution profile. Our finding that in resting, healthy animals, the plasma VWF multimer distribution in WT and *Tsp1*$^{-/-}$ mice is identical, may reflect the existence of ADAMTS13-independent release in the bloodstream in normal physiologic conditions.

Nevertheless, TSP-1 has structural homology to ADAMTS13[44] and, like the latter, binds to the A3 domain of VWF.[19] Our present findings in flow studies over endothelial cells confirm that TSP-1 interferes with recombinant ADAMTS13 for binding to ultralarge VWF multimers and therefore inhibits VWF cleavage, a finding also valid for plasma ADAMTS13. In contrast to the VWF multimer analysis in plasma at rest, those assays are reminiscent of conditions reflecting enhanced vascular activity, such as endothelial cell inflammation accompanied by Weibel-Palade release and endothelial denudation, exposing subendothelial VWF and platelet-released ultralarge VWF molecules.

We found, indeed, in WT and in *Tsp1*$^{-/-}$ mouse mesenteric blood vessels, that ultralarge VWF multimers form immediately upon endothelial cell activation, leading to tethering and firm adhesion of fluorescently labeled platelets, which also results in platelet string formation on the endothelium. Platelet string formation was affected in *Tsp1*-null mice, but platelet interactions with *Tsp1*$^{-/-}$ endothelium were restored both by neutralization of ADAMTS13 and by treatment with TSP-1, substantiating that already low concentrations of TSP-1 (formally 1 μg/mL) shield endothelial-exposed VWF from degradation by ADAMTS13. The finding in WT mice that platelet-endothelial interactions can be stimulated moderately by TSP-1 and anti-ADAMTS13 antibodies is in agreement with incomplete shielding of VWF by the low TSP-1 plasma levels, for degradation by circulating ADAMTS13, in resting conditions. Similarly to the role of ADAMTS13 in the control of endothelially derived VWF, the enhanced embolization of thrombi observed in *Tsp1*$^{-/-}$ mice will therefore result from defective protection by TSP-1 of unfolded subendothelial VWF involved in thrombus attachment, which appears to be degraded by ADAMTS13. The similar correction of this phenotype by TSP-1 and by neutralizing ADAMTS13 antibodies indeed confirms that ADAMTS13 is capable of slowly degrading VWF at the interface between the thrombus and the vessel wall, even when it is not in direct contact with the bloodstream. It is imaginable that VWF is stretched by tensile forces while retaining a growing thrombus in a field of shear forces, similar to the execution of shear forces on VWF strings by the attached platelets.[47]

This interpretation is compatible with the large TSP-1 content of platelets. Upon exposure to the circulation of subendothelial VWF, and following platelet adhesion, platelet activation triggers the local release of high concentrations of TSP-1, protecting subendothelial VWF from degradation. During thrombus formation, in addition to releasing TSP-1, activated platelets also secrete large VWF multimers, which may likewise be protected from cleavage by ADAMTS13, thus contributing to thrombus stabilization.

Low concentrations of TSP-1 restored the embolization phenotype in *Tsp1*-null mice and had no effect in WT controls. However, when administered at high concentrations to *Tsp1*-null mice, TSP-1 shortened occlusion times to values below those found in WT controls (Figure 8). The present study therefore suggests that the complete prevention of ADAMTS13-mediated VWF (sub)endothelial trimming by high plasma concentrations of TSP-1 may predispose humans to thrombosis. Clinical correlations so far have suggested that a missense TSP-1 variant (N700S) in premature myocardial infarction was associated with an adjusted odds ratio for coronary artery disease of 11.9 in homozygous individuals, but such individuals were found to have low plasma TSP-1 levels.[17] Therefore, TSP-1 plasma levels will have to be studied in more detail in cohorts of cardiovascular patients to determine whether TSP-1 plasma levels correlate with thrombophilia. Such investigations should accompany mutational analyses and screening for gain-of-function or loss-of-function mutations in this multifunctional protein.

In summary, no evidence was found for a role for TSP-1 in platelet aggregation or in coagulation-mediated thrombosis, but our work demonstrates a role for TSP-1 in platelet recruitment to stimulated endothelium and in thrombus stabilization in vivo by securing platelet and thrombus adhesiveness to shear stress–operated VWF through protection of (sub)endothelial VWF cleavage by ADAMTS13.

References

1. Ruggeri ZM. Mechanisms initiating platelet thrombus formation. Thromb Haemost. 1997;78:611-616.
2. Ware J, Ruggeri ZM. Platelet adhesion receptors and their participation in hemostasis and thrombosis. Drugs Today (Barc). 2001;37:265-274.
3. Ni H, Denis CV, Subbarao S, et al. Persistence of platelet thrombus formation in arterioles of mice lacking both von Willebrand factor and fibrinogen. J Clin Invest. 2000;106:385-392.
4. Ni H, Yuen PS, Papalia JM, et al. Plasma fibronectin promotes thrombus growth and stability in injured arterioles. Proc Natl Acad Sci U S A. 2003;100:2415-2419.
5. Tuszynski GP, Nicosia RF. The role of thrombospondin-1 in tumor progression and angiogenesis. Bioessays. 1996;18:71-76.
6. Dubernard V, Arbeille BB, Lemesle MB, Legrand

C. Evidence for an alpha-granular pool of the cytoskeletal protein alpha-actinin in human platelets that redistributes with the adhesive glycoprotein thrombospondin-1 during the exocytotic process. Arterioscler Thromb Vasc Biol. 1997;17:2293-2305.

7. Lawler J, Duquette M, Urry L, McHenry K, Smith TF. The evolution of the thrombospondin gene family. J Mol Evol. 1993;36:509-516.
8. Legrand C, Thibert V, Dubernard V, Begault B, Lawler J. Molecular requirements for the interaction of thrombospondin with thrombin-activated human platelets: modulation of platelet aggregation. Blood. 1992;79:1995-2003.
9. Legrand C, Morandi V, Mendelovitz S, Shaked H, Hartman JR, Panet A. Selective inhibition of platelet macroaggregate formation by a recombinant heparin-binding domain of human thrombospondin. Arterioscler Thromb. 1994;14:1784-1791.
10. Bonnefoy A, Hantgan R, Legrand C, Frojmovic MM. A model of platelet aggregation involving multiple interactions of thrombospondin-1, fibrinogen, and GPIIbIIIa receptor. J Biol Chem. 2001; 276:5605-5612.
11. Chung J, Gao AG, Frazier WA. Thrombspondin acts via integrin-associated protein to activate the platelet integrin alphaIIbbeta3. J Biol Chem. 1997;272:14740-14746.
12. Chung J, Wang XQ, Lindberg FP, Frazier WA. Thrombospondin-1 acts via IAP/CD47 to synergize with collagen in alpha2beta1-mediated platelet activation. Blood. 1999;94:642-648.
13. Frazier WA, Gao AG, Dimitry J, et al. The thrombospondin receptor integrin-associated protein (CD47) functionally couples to heterotrimeric Gi. J Biol Chem. 1999;274:8554-8560.
14. Jurk K, Clemetson KJ, de Groot PG, et al. Thrombospondin-1 mediates platelet adhesion at high shear via glycoprotein Ib (GPIb): an alternative/backup mechanism to von Willebrand factor. FASEB J. 2003;17:1490-1492.
15. Lagadec P, Dejoux O, Ticchioni M, et al. Involvement of a CD47-dependent pathway in platelet adhesion on inflamed vascular endothelium under flow. Blood. 2003;101:4836-4843.
16. Lawler J, Sunday M, Thibert V, et al. Thrombospondin-1 is required for normal murine pulmonary homeostasis and its absence causes pneumonia. J Clin Invest. 1998;101:982-992.
17. Topol EJ, McCarthy J, Gabriel S, et al. Single nucleotide polymorphisms in multiple novel thrombospondin genes may be associated with familial premature myocardial infarction. Circulation. 2001;104:2641-2644.
18. Zhao XM, Hu Y, Miller GG, Mitchell RN, Libby P. Association of thrombospondin-1 and cardiac allograft vasculopathy in human cardiac allografts. Circulation. 2001;103:525-531.
19. Pimanda JE, Ganderton T, Maekawa A, et al. Role of thrombospondin-1 in control of von Willebrand factor multimer size in mice. J Biol Chem. 2004;279:21439-21448.
20. Dubernard V, Legrand C. Characterization of the binding of thrombospondin to human platelets and its association with the platelet cytoskeleton. J Lab Clin Med. 1991;118:446-457.
21. Veyradier A, Girma JP. Assays of ADAMTS-13 activity. Semin Hematol. 2004;41:41-47.
22. Theilmeier G, Lenaerts T, Remacle C, Collen D, Vermylen J, Hoylaerts MF. Circulating activated platelets assist THP-1 monocytoid/endothelial cell interaction under shear stress. Blood. 1999; 94:2725-2734.
23. Theilmeier G, Michiels C, Spaepen E, et al. Endothelial von Willebrand factor recruits platelets to atherosclerosis-prone sites in response to hypercholesterolemia. Blood. 2002;99:4486-4493.
24. Giles AR. Guidelines for the use of animals in biomedical research. Thromb Haemost. 1987;58: 1078-1084.
25. Oury C, Kuijpers MJ, Toth-Zsamboki E, et al. Overexpression of the platelet P2X1 ion channel in transgenic mice generates a novel prothrombotic phenotype. Blood. 2003;101:3969-3976.
26. André P, Denis CV, Ware J, et al. Platelets adhere to and translocate on von Willebrand factor presented by endothelium in stimulated veins. Blood. 2000;96:3322-3328.
27. Vanschoonbeek K, Feijge MA, Van Kampen RJ, et al. Initiating and potentiating role of platelets in tissue factor-induced thrombin generation in the presence of plasma: subject-dependent variation in thrombogram characteristics. J Thromb Haemost. 2004;2:476-484.
28. Dong JF, Moake JL, Nolasco L, et al. ADAMTS-13 rapidly cleaves newly secreted ultralarge von Willebrand factor multimers on the endothelial surface under flowing conditions. Blood. 2002;100:4033-4039.
29. Dong JF, Moake JL, Bernardo A, et al. ADAMTS-13 metalloprotease interacts with the endothelial cell-derived ultra-large von Willebrand factor. J Biol Chem. 2003;278:29633-29639.
30. Mast AE, Stadanlick JE, Lockett JM, Dietzen DJ, Hasty KA, Hall CL. Tissue factor pathway inhibitor binds to platelet thrombospondin-1. J Biol Chem. 2000;275:31715-31721.
31. McGregor JL, Catimel B, Parmentier S, Clezardin P, Dechavanne M, Leung LL. Rapid purification and partial characterization of human platelet glycoprotein IIIb: interaction with thrombospondin and its role in platelet aggregation. J Biol Chem. 1989;264:501-506.
32. Lawler J, Weinstein R, Hynes RO. Cell attachment to thrombospondin: the role of ARG-GLY-ASP, calcium, and integrin receptors. J Cell Biol. 1988;107:2351-2361.
33. Lawler J, Hynes RO. An integrin receptor on normal and thrombasthenic platelets that binds thrombospondin. Blood. 1989;74:2022-2027.
34. Gao AG, Lindberg FP, Finn MB, Blystone SD, Brown EJ, Frazier WA. Integrin-associated protein is a receptor for the C-terminal domain of thrombospondin. J Biol Chem. 1996;271:21-24.
35. Hogg PJ. Thrombospondin 1 as an enzyme inhibitor. Thromb Haemost. 1994;72:787-792.
36. Boukerche H, McGregor JL. Characterization of an anti-thrombospondin monoclonal antibody (P8) that inhibits human blood platelet functions: normal binding of P8 to thrombin-activated Glanzmann thrombasthenic platelets. Eur J Biochem. 1988;171:383-392.
37. Dixit VM, Haverstick DM, O'Rourke KM, et al. A monoclonal antibody against human thrombospondin inhibits platelet aggregation. Proc Natl Acad Sci U S A. 1985;82:3472-3476.
38. Dixit VM, Haverstick DM, O'Rourke KM, et al. Effects of anti-thrombospondin monoclonal antibodies on the agglutination of erythrocytes and fixed, activated platelets by purified thrombospondin. Biochemistry. 1985;24:4270-4275.
39. Vailhe B, Feige JJ. Thrombospondins as anti-angiogenic therapeutic agents. Curr Pharm Des. 2003;9:583-588.
40. Calzada MJ, Zhou L, Sipes JM, et al. $\alpha 4\beta 1$ integrin mediates selective endothelial cell responses to thrombospondins 1 and 2 in vitro and modulates angiogenesis in vivo. Circ Res. 2004;94:462-470.
41. Rybak ME. Glycoproteins IIb and IIIa and platelet thrombospondin in a liposome model of platelet aggregation. Thromb Haemost. 1986;55:240-245.
42. Leung LL. Role of thrombospondin in platelet aggregation. J Clin Invest. 1984;74:1764-1772.
43. Padilla A, Moake JL, Bernardo A, et al. P-selectin anchors newly released ultra-large von Willebrand factor multimers to the endothelial cell surface. Blood. 2003;103:2150-2156.
44. Lopez JA, Dong JF. Cleavage of von Willebrand factor by ADAMTS-13 on endothelial cells. Semin Hematol. 2004;41:15-23.
45. Lammle B, Kremer Hovinga JA, Alberio L. Thrombotic thrombocytopenic purpura. J Thromb Haemost. 2005;3:1663-1675.
46. Paleolog EM, Crossman DC, McVey JH, Pearson JD. Differential regulation by cytokines of constitutive and stimulated secretion of von Willebrand factor from endothelial cells. Blood. 1990;75:688-695.
47. Dong JF. Cleavage of ultra-large von Willebrand factor by ADAMTS-13 under flow conditions. J Thromb Haemost. 2005;3:1710-1716.